

## Article

# Screening of Haustorium Induction Factors of *Phelipanche aegyptiaca* Pers. Based on Metabolome Analysis of *Cucumis melo* L. Root Exudates

Pengxuan Bian, Chang Sun, Xiaolei Cao, Zhaoqun Yao, Xuekun Zhang \* and Sifeng Zhao \*

Key Laboratory at the Universities of Xinjiang Uygur Autonomous Region for Oasis Agricultural Pest Management and Plant Protection Resource Utilization, Agriculture College, Shihezi University, Shihezi 832003, China

\* Correspondence: zhangxk2459@163.com (X.Z.); zhsf\_agr@shzu.edu.cn (S.Z.)

**Abstract:** *Phelipanche aegyptiaca* Pers. is a holoparasitic plant that causes tremendous losses of agricultural crops worldwide. The initiation and development of the haustoria (special intrusive organs) is a key step in the growth of parasitic plants. The initiation of haustorium is largely dependent on haustorium-inducing factors (HIFs) secreted from host roots. Although HIFs of many semi-parasitic plants have been identified and reported, HIFs of the obligate parasitic plant *P. aegyptiaca* are largely unknown. This work demonstrated that the root exudates of the host plant *Cucumis melo* L. contain allelochemicals displaying haustorium-inducing activity on *P. aegyptiaca* germinating seeds, and there are significant differences in the induction effects of the resistant and susceptible *C. melo* cultivars of *P. aegyptiaca* (KR1326 and K1076). Ultra-performance liquid chromatography–mass spectrometry (UPLC-MS/MS) technology was used to identify and analyze the metabolites in root exudates of KR1326 and K1076. Cluster and PCA analyses showed significant differences between the metabolites in the KR1326 and K1076 root exudates. The determination of the haustorium induction effects of some metabolites screened from the differential metabolites indicated that scopoletin, quercetin, IAA, and DMBQ had relatively high haustorium induction activity. The results provide clues for finding HIFs of obligate parasitic plants and shed new light on the control of *P. aegyptiaca* by regulating haustorium development.

**Keywords:** *Cucumis melo*; *Phelipanche aegyptiaca*; haustorium; root exudates; widely targeted metabonomics



**Citation:** Bian, P.; Sun, C.; Cao, X.; Yao, Z.; Zhang, X.; Zhao, S. Screening of Haustorium Induction Factors of *Phelipanche aegyptiaca* Pers. Based on Metabolome Analysis of *Cucumis melo* L. Root Exudates. *Agronomy* **2023**, *13*, 128. <https://doi.org/10.3390/agronomy13010128>

Academic Editor: Natividad Chaves Lobón

Received: 13 November 2022

Revised: 20 December 2022

Accepted: 27 December 2022

Published: 30 December 2022

Corrected: 20 October 2023



**Copyright:** © 2022 by the authors. Licensee MDPI, Basel, Switzerland. This article is an open access article distributed under the terms and conditions of the Creative Commons Attribution (CC BY) license (<https://creativecommons.org/licenses/by/4.0/>).

## 1. Introduction

*Phelipanche aegyptiaca* is an annual root parasitic weed that is widely distributed in temperate and subtropical regions of the Mediterranean, southern and northern Africa, eastern and southern Europe, and South Asia [1–3]. This parasite of the Orobanchaceae family is one of the most harmful to agricultural crops worldwide. In China, *P. aegyptiaca* has spread almost all over Xinjiang, severely affecting the production of the main crops, such as tomato, melon, and sunflower. It has given rise to a large area of production reduction, or even almost no harvest, causing a loss of more than CNY 500 million to the local area each year [4,5]. Hence, the prevention and control of *P. aegyptiaca* is in an important position. As an obligate parasitic weed, *P. aegyptiaca* parasitizes the roots of host crops to obtain water and nutrients through the haustoria, affecting the normal growth of crops and causing agricultural losses. Due to the huge seed bank of *P. aegyptiaca* in the soil and its unique parasitic characteristics, traditional agricultural and chemical methods do not effectively control its hazards. Therefore, blocking the nutrient absorption channel and reducing the harm of *P. aegyptiaca* to the host are of great scientific significance for its control.

The life cycle of *P. aegyptiaca* is the same as the majority of the holoparasitic Orobanchaceae, including the seed phase, the autotrophic growth phase, and the heterotrophic

growth phase. In the seed phase, the seeds of *P. aegyptiaca* dormant in the soil to form a huge seed bank, which germinated after responding to allelochemicals, such as strigolactones (SLs) secreted by the host roots, and then enter in an autotrophic growth phase. Subsequently, the radicle of *P. aegyptiaca* tends to grow toward the host root and forms terminal haustorium under the induction of HIFs when approaching the host root. Then *P. aegyptiaca* invaded the host by means of the haustorium, established the parasitic relationship, and entered the heterotrophic growth phase [1,6]. Thus it can be seen that the haustorium is the special organ of parasitic plants, and its formation is a critical step for the transition from an autotrophic to a heterotrophic lifestyle [7]. Obligate parasitic plant *P. aegyptiaca* forms terminal haustoria to attach and penetrate the host root and obtain sugars, water, and other nutrients required for life by developing the vascular connection between the parasite and the host, thus causing damage to host growth and development [8]. In addition, haustoria are also an important channel for material exchange and information communication between hosts and parasites, such as viruses, siRNAs, nucleic acids, and proteins, which are transferred between the parasite and host through the haustoria [9–12]. Therefore, the haustorium initiation and development are crucial steps in the lifecycle of parasitic plants [1,7,13]. Nevertheless, haustorium initiation is not spontaneous during the growth of parasitic plants; only contact with host- or non-host-exudated chemical stimulation under appropriate temperatures and humidity conditions can trigger haustorium initiation and development. The chemicals that induce haustorium initiation in the Orobanchaceae are called haustorium-inducing factors (HIFs) [7]. Searching for HIFs is helpful in understanding the haustorium formation of parasitic plants and in applying it to the control of *P. aegyptiaca*. However, their synthetic pathways and specific sources are largely unknown. Numerous studies have shown that the root exudates of numerous plant species can induce prehaustoria [7,14–16]. The root exudates extracted from the highly susceptible *Brassica napus* cultivar had a high induction activity for the haustorium formation of *Phelipanche ramosa*, and parasite aggressiveness was significantly enhanced after treatment with root exudates [14]. Root exudates and tissue extracts of rice and *Arabidopsis* can induce *Phtheirospermum japonicum* and *Striga hermonthica* haustorium formation [15], which confirmed that host root exudates contain HIFs of parasitic plants. In 2022, the planting area of *Cucumis melo* L. in Xinjiang was 626,500 hectares, with a total output of 2,116,600 tons, as an important economic crop in Xinjiang, *C. melo* has been seriously damaged by *P. aegyptiaca*. Although it is one of the main hosts of *P. aegyptiaca*, the effects of its root exudates on the germination and haustorium development of *P. aegyptiaca* have not been reported. The interaction mechanism between *C. melo* root exudates and *P. aegyptiaca* haustorium is also unknown.

At present, an increasing number of allelochemicals have been found and extracted from plant root exudates, and the haustorial induction activity of individual allelochemicals has been determined. It has been reported that the types of parasitic plant HIFs in plant root exudates mainly include phenolic acids, quinones, flavonoids, lignin units, cytokinins, and cyclohexene oxides [13], which show different haustorial induction activities for different parasitic plant species. The first HIF discovered, 2,6-dimethoxybenzoquinone (DMBQ), was isolated from sorghum roots and shown to trigger haustorium formation in *Triphysaria versicolor* and *Striga hermonthica* [16,17]. Compounds with structures similar to DMBQ, such as phenolic acids (including syringic acid, vanillic acid, and ferulic acid), aldehydes (including syringaldehyde), and flavonoids (including peonidin), have also been reported to induce haustoria in *Triphysaria versicolor*, *Phtheirospermum japonicum*, and *Striga hermonthica* [15]. The mycotoxins sphaeropsidone and epi-sphaeropsidone, which are cyclohexene oxides isolated from *Diplodia cupressi*, the causal agent for cypress (*Cupressus sempervirens* L.) canker, have HIF activity in vitro toward *Orobanche crenata* and *O. cumana* [18,19]. Treatments with phytohormones also trigger haustorium formation. In addition, auxin efflux activity within the haustoria at later developmental stages is crucial for xylem bridge formation [20]. Ethylene signaling in the parasite is crucial for the haustorium apex cells to differentiate into intrusive cells for host invasion. While the exogenous application of ethylene suppresses

haustorium development, ethylene signaling is dispensable during early haustorium initiation, but is required for the timely termination of haustorium growth in the absence of a host [21]. Nitrogen increases the levels of abscisic acid (ABA) in *P. japonicum* and prevents the activation of hundreds of genes, including cell cycle and xylem development genes. Blocking ABA signaling overcomes nitrogen's inhibitory effects, indicating that nitrogen represses haustoria formation by increasing ABA [22]. Cytokinins constitutively exuded from host roots play a major role in haustorium formation and aggressiveness in *P. ramosa* [14]. In addition, ROS and ROS-regulating enzymes are indispensable in the downstream signaling of HIFs for haustorium formation [23]. In *P. japonicum*, DMBQ initiates  $\text{Ca}^{2+}$  signaling in the root and is important for the development of the haustorium [24]. However, the regulation of these allelochemicals and pathways on *P. aegyptiaca* haustorium has not been reported.

Here, based on the resistant and susceptible *C. melo* cultivars KR1326 and K1076, respectively, obtained by previous research, there was a significant difference in the induction effect of root exudates of KR1326 and K1076 on seed germination and haustorium formation. Using widely targeted metabolomics based on ultra-high performance liquid chromatography–tandem mass spectrometry (UPLC-MS/MS) technology, the metabolites in root exudates of *P. aegyptiaca* were analyzed and identified. Through multivariate statistical analysis methods, such as principal component analysis (PCA) and orthogonal partial least squares discriminant analysis (OPLS-DA), the differential metabolites in the root exudates of KR1326 and K1076 were screened, and the haustorium induction activity of allelochemicals that could be used as potential HIFs was tested. Thus, the allelochemicals in *C. melo* root exudates that can be used as HIFs of *P. aegyptiaca* were screened. This sheds new light on the control of *P. aegyptiaca* by regulating the haustorium development and provides clues for determining the mechanisms by which parasitic plants respond to host root-derived molecules.

## 2. Materials and Methods

### 2.1. Plant Materials and Growth Conditions

In 2020, the seeds of *P. aegyptiaca* were collected from tomato fields in Jimusar County, Xinjiang province, China. These seeds were stored at 25 °C in the dark before use. *Cucumis melo* L. cultivars KR1326 (resistant) and K1076 (susceptible) were provided by the Hami Melon Research Center, Xinjiang Academy of Agricultural Sciences. *Cucumis melo* seeds were surface-sterilized using 2% (*v/v*) sodium hypochlorite and germinated in sterilized water for 2 days. Germinated seeds were planted in a 50-hole (5 × 5 × 5 cm) plastic cave dish containing vermiculite medium, grown in a growth chamber at 25 °C with a photoperiod of 16-h light and 8-h dark for 10 days, and regularly watered once every two days. *Cucumis melo* seedlings with one fully developed true leaf were transferred to a black hydroponic box [1200 mL, 15 × 20 × 7 cm (W × L × H)] filled with 1000 mL Hoagland nutrient solution (Table S5). After rinsing the root with sterilized water at least three times, fresh nutrient solution was supplied every 3 days. *Phelipanche aegyptiaca* seeds were sterilized with 75% (*v/v*) ethanol for 2 min and 2% (*v/v*) sodium hypochlorite for 15 min and then rinsed with sterilized water at least 5 times. Pre-conditioning, germination, and haustorium induction of *P. aegyptiaca* seeds were performed in an incubator (A1000, CONVIRON, Winnipeg, MB, Canada) at 25 °C in the dark.

### 2.2. Collection and Treatment of Root Exudates

The root exudates were collected from *C. melo* seedlings at the flowering stage (33 days old) by means of hydroponic culture. To collect root exudates, six *C. melo* plants were moved to a clean hydroponic box filled with 300 mL sterilized water at 25 °C with a photoperiod of 16 h light and 8 h dark for 24 h. Three replicate samples were prepared for each experiment. The aqueous solution was collected from the hydroponic box and centrifuged (12,000 r/min, 4 °C) for 10 min. The supernatant was then immediately concentrated to 10 mL in a rotary evaporator (RV 10 D S96, IKA, Königswinter, Germany). Concentrated root exudates were

used for *P. aegyptiaca* seed germination and haustorium induction after filtering with a microporous filter membrane (0.45  $\mu\text{m}$ ).

For metabolite extraction, 9 mL of each sample was placed in a 50-mL centrifuge tube after mixing, and the samples were immersed in liquid nitrogen. The samples were freeze-dried in a lyophilizer (SCIENTZ-12N/D, Zhejiang, China) after being completely frozen. Then, 300  $\mu\text{L}$  of 70% methanol internal standard extract was added and scrolled for 15 min. The samples were then centrifuged (12,000 r/min, 4  $^{\circ}\text{C}$ ) for 3 min. The supernatant was filtered with a microporous filter membrane (0.22  $\mu\text{m}$ ) and stored in a sample flask for UPLC-MS/MS.

### 2.3. Quantification of Seed Germination and Haustorium Induction

For pre-conditioning, 100 *P. aegyptiaca* seeds were evenly placed on a Petri dish with two pieces of moistened filter paper after surface sterilization and incubated at 25  $^{\circ}\text{C}$  in the dark for 5 days. For seed germination, *P. aegyptiaca* seeds were treated with 1 mL of root exudates for 6 days after pre-conditioning. GR24 has been widely used in the seed germination of *Orobance* [25,26] and thus was used as a positive control.

For haustorium induction, after rac-GR24 ( $1 \times 10^{-7}$  mol/L) treatment for 3 days, germinated *P. aegyptiaca* seedlings were induced with *C. melo* root exudates and each chemical compound (Table S1) for 7 days before quantifying haustoria directly with a stereomicroscope (ZEISS AxioCam ICc 5, Baden-Württemberg, Germany). One *P. aegyptiaca* seed can form only one terminal haustorium, developing a swollen and multicellular structure in the root apex (Figure 1C). Therefore, we used the number of seeds that formed an obvious haustorium structure characteristic to measure the haustorium induction rate of each chemical by calculating the percentage of haustorium formation in *P. aegyptiaca* seeds after treatment with different concentrations of each compound (Table S1).

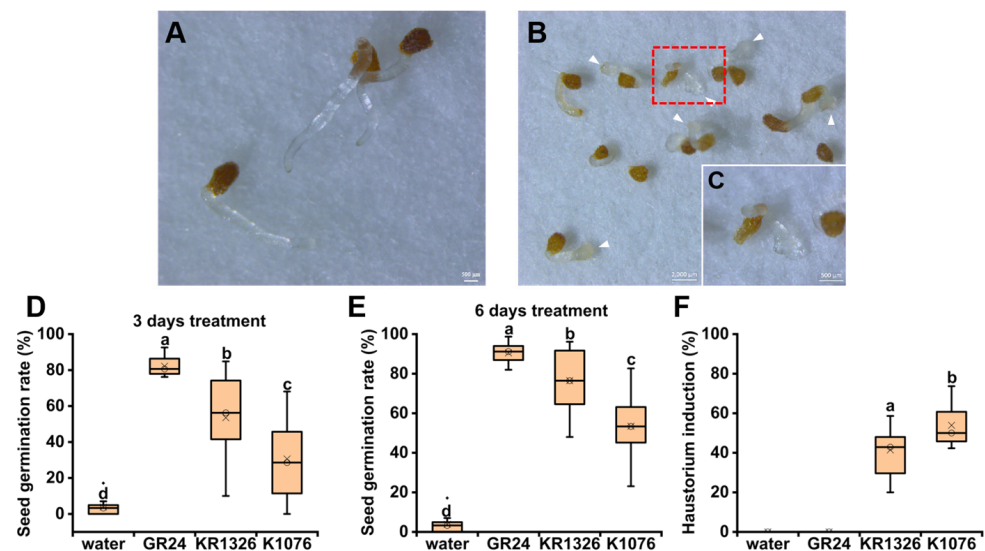


**Figure 1.** *C. melo* root exudates can induce the weed's germination and haustorium formation in *P. aegyptiaca*. (A–C) Germinated seeds and haustorium formation of *P. aegyptiaca* induced by *C. melo* root exudates on filter paper in a Petri dish. (D,F) Seed germination and haustorium induction rate of *P. aegyptiaca* induced by *C. melo* root exudates. (A) *P. aegyptiaca* seeds treated with GR24 for 6 days displayed a thin and regular conical apex. (B) Representative image showing haustorium formation at the root tip of *P. aegyptiaca* seedlings after KRI326 root exudate treatment for 7 days. White triangle marks: the swollen and irregular multicellular structure at the apex of *P. aegyptiaca* radicle. Red box marks: Representative image showing haustorium structure. (C) Representative image showing haustorium structure. Enlarged view of the white box in (B). (D) Seeds germination rate treated by root exudates for 3–6 days. (E) Haustorium induction rate treated with root exudates for 7 days.

Seven metabolites were selected from the differential metabolites to evaluate their haustorium-inducing activity. According to previous studies, host-mediated cytokinins, ethylene signal, and auxin efflux activity play an important role in the regulation of haustorium formation [25,26]; therefore, the cytokinins auxin and ethephon were also applied for the haustorium induction of *P. aegyptiaca*. DMBQ has been widely used as a HIF in hemi-parasitic plants and thus was tested for haustorium induction activity in *P. aegyptiaca*. Root exudates were confirmed to have haustorium-inducing activity in this study, so the mixed root exudates of the two cultivars were used as positive controls to evaluate the haustorium activity of different chemical compounds. GR24 and sterilized water were treated separately as negative controls. Each chemical treatment was accompanied by the corresponding solvent as a control to evaluate whether the solvent had a negative effect on *P. aegyptiaca* development. At least three biological replicates per treatment and 30 *P. aegyptiaca* seeds were measured per replicate.

#### 2.4. Conditions for the Analysis of UPLC-MS/MS

Metabolite analysis was sequentially processed at Wuhan Metware Biotechnology Co., Ltd. ([www.metware.cn](http://www.metware.cn), accessed on 6 February 2022). The sample extracts were analyzed using an UPLC-ESI-MS/MS system (UPLC, SHIMADZU Nexera X2; MS, Applied Biosystems 4500 Q TRAP, Waltham, MA, USA).

The UPLC analytical conditions were as follows: UPLC: column, Agilent SB-C18 (1.8  $\mu\text{m}$ , 2.1 mm  $\times$  100 mm); the mobile phase consisted of solvent A, pure water with 0.1% formic acid, and solvent B was acetonitrile with 0.1% formic acid. Sample measurements were performed with a gradient program that employed the starting conditions of 95% A and 5% B. Within 9 min, a linear gradient to 5% A and 95% B was programmed, and a composition of 5% A and 95% B was maintained for 1 min. Subsequently, a composition of 95% A and 5.0% B was adjusted within 1.1 min and kept for 2.9 min. The flow velocity was set as 0.35 mL per min; the column oven was set to 40  $^{\circ}\text{C}$ ; the injection volume was 4  $\mu\text{L}$ . The effluent was alternatively connected to an ESI-triple quadrupole-linear ion trap (QTRAP)-MS.

The ESI-Q TRAP-MS/MS analytical conditions were as follows: LIT and triple quadrupole (QQQ) scans were acquired on a triple quadrupole-linear ion trap mass spectrometer (Q TRAP), AB4500 Q TRAP UPLC/MS/MS System, equipped with an ESI Turbo Ion-Spray interface, operating in positive and negative ion mode and controlled by Analyst 1.6.3 software (AB Sciex, Framingham, MA, USA). The ESI source operation parameters were as follows: ion source, turbo spray; source temperature 550  $^{\circ}\text{C}$ ; ion spray voltage (IS) 5500 V (positive ion mode)/−4500 V (negative ion mode); ion source gas I (GSI), gas II (GSII), and curtain gas (CUR) were set at 50, 60, and 25.0 psi, respectively; collision-activated dissociation (CAD) was high. Instrument tuning and mass calibration were performed with 10 and 100  $\mu\text{mol/L}$  polypropylene glycol solutions in the QQQ and LIT modes, respectively. QQQ scans were acquired as MRM experiments with collision gas (nitrogen) set to medium. Declustering potential (DP) and collision energy (CE) for individual MRM transitions were performed with further DP and CE optimization. A specific set of MRM transitions was monitored for each period, according to the metabolites eluted within this period.

#### 2.5. Qualitative and Quantitative Determination of Metabolites

Based on the self-built database MWDB (Metware Biotechnology Co., Ltd., Wuhan, China) and the public database of metabolite information, secondary mass spectrometry data were subjected to qualitative analysis. To avoid interference, isotope signals, duplicate signals of  $\text{K}^+$ ,  $\text{Na}^+$ , and  $\text{NH}_4^+$  ions, and duplicate signals of fragment ions derived from other relatively large molecules were excluded.

Metabolite quantification was performed using the MRM mode of the QQQ mass spectrometer. In the MRM mode, the quadrupole first screened the precursor ions (parent ions) of the target substances and removed the corresponding ions of other substances with different molecular weights to eliminate interference preliminarily. The precursor

ions were fragmented via induced ionization in the collision chamber to form many fragment ions, which were then filtered through QQQ to select single-fragment ions with the desired characteristics while eliminating interference from non-target ions, leading to the increased precision and repeatability of the quantification results. After the metabolite mass spectrometry data were obtained for the different samples, all mass spectrum peaks were subjected to area integration, and the mass spectra peaks of the same metabolite in the different samples were integrated and corrected using MultiaQuant software (Sciex, Framingham, MA, USA). The area of each peak represented the relative content of the corresponding substance.

### 2.6. Data Analysis

Multivariate statistical analysis methods, namely, principal component analysis (PCA) and orthogonal partial least squares-discriminant analysis (OPLS-DA), were used to process the metabolic data. PCA was first carried out on all samples, including quality control samples (QC), to elucidate the total metabolic differences and degree of variation among the samples. Fold change (FC) and variable importance in projection (VIP) values of the orthogonal partial least squares discriminant analysis (OPLS-DA) model were used to screen differential metabolites. The accumulation pattern of metabolites among different samples was analyzed by cluster analysis with R software version 2.8.0, ([www.r-project.org/](http://www.r-project.org/), accessed on 25 February 2022). The Kyoto Encyclopedia of Genes and Genomes (KEGG) database was used to annotate and enrich differential metabolites.

The obtained experimental data were subjected to a one-way analysis of variance (ANOVA) using IBM SPSS Statistics V22. The mean values of the tested treatments were compared using the least significant range (L.S.R.) according to Duncan's multiple range test at a  $p = 0.05$  level of probability. Figures were drawn using Origin 2021 and Rstudio Version 1.3.1093 (Boston, MA, USA).

## 3. Results

### 3.1. Effects of *C. melo* Root Exudates on Seed Germination and Haustorium Induction of *P. aegyptiaca*

Root exudates from two *C. melo* cultivars showed significant activity in seed germination and haustorium induction. Germinated seeds were observed after 24 h of treatment with root exudates. The seed germination rates were investigated on the third and sixth days. On the third day after treatment, the seed germination rates of KR1326 and K1076 were 53.54% and 30.60%, respectively. On the sixth day after treatment, the seed germination rates of KR1326 and K1076 reached 76.48% and 53.46%, respectively. The seed germination rate of KR1326 was significantly higher than that of K1076 both on the third and sixth days. However, the germination rate of seeds treated with root exudates was significantly lower than that of the positive control on both the third and sixth days (Figure 1D,E). Treatment with sterilized water (Mock) alone hardly induced the germination of *P. aegyptiaca* weeds (Figure 1D).

The same methods were used to induce *P. aegyptiaca* haustoria and to assess the haustorium-inducing activity of *C. melo* root exudates. The swollen and irregular multicellular structures, typical characteristics of the haustorium of obligate parasitic plants, were observed at the apex of the radicles in the KR1326 and K1076 root exudate treatments. Meanwhile, the radicles were relatively short, indicating that elongation was blocked (Figure 1B,C). However, with no haustorium formation in GR24 and sterilized water treatment, the normal growing radicles were relatively long and displayed thin and shaped conical apices (Figure 1A). The haustorium induction rate was investigated on the seventh day after treatment. The haustorium induction rates of KR1326 and K1076 were 41.47% and 53.90%, respectively. Interestingly, the haustorium induction rate of K1076 was significantly higher than that of KR1326 (Figure 1F).

### 3.2. Widely Targeted Metabolome Analysis of *C. melo* Root Exudates

To explore the reasons for the difference in the haustorium induction activity of resistant and susceptible *C. melo* root exudates, searching for potential HIFs in *C. melo* root exudates, six samples from resistant and susceptible *C. melo* cultivars were selected to study the differences in variety and content in metabolites using UPLC-MS/MS analysis. Based on widely targeted metabolomics, 675 metabolites were detected in the metabolic analysis. To check the quality of the acquired MS data, an MRM metabolite detection multi-peak map and total ion chromatogram (TIC) were generated and analyzed, revealing a high degree of overlap and a good sample preparation process (Figure 2A,B). The PCA of the profiles of these 675 metabolite features indicated that the root exudates of KR1326 were clearly separated from those of K1076 (Figure 2E), indicating that the metabolite profiles of KR1326 root exudates are markedly different from those of K1076. An overview of the metabolite profiling of *C. melo* root exudates is shown in Table S2. All identified metabolites were divided into 11 categories (Figure 2D). Among them, lipids (136 metabolites), amino acid derivatives (83 metabolites), and phenolic acids (79 metabolites) represented the most metabolites. The total changes in the metabolite content among the root exudate samples were visualized using heatmap cluster analysis (Figure 2C). According to the change in color depth in the picture, it can be seen intuitively that there was a significant difference in the metabolite content between the root exudates of KR1326 and K1076.

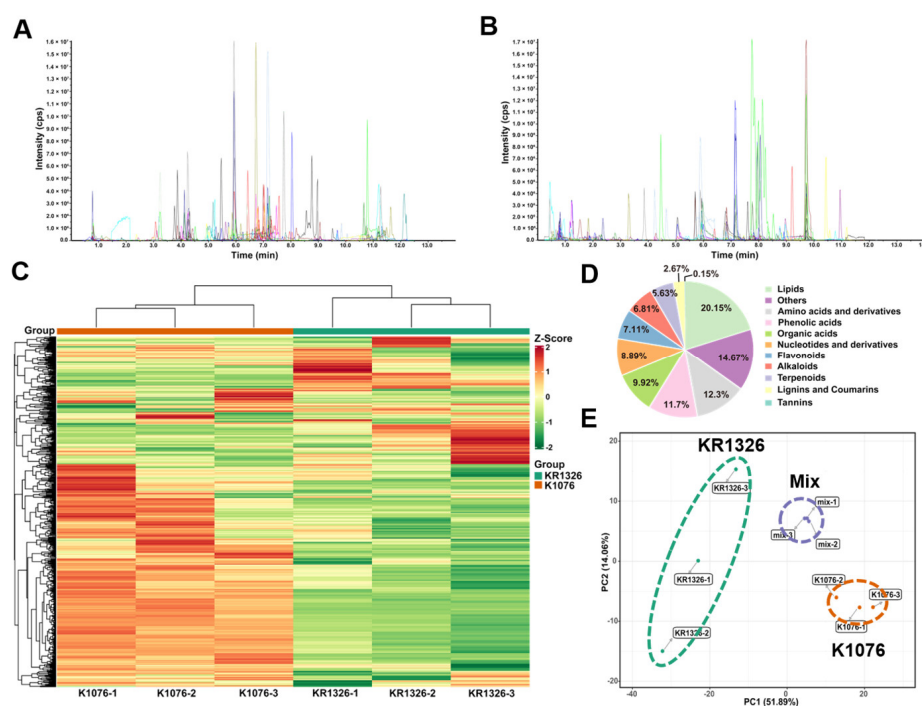


**Figure 2.** Widely targeted metabolite profiling reveals the metabolites in *C. melo* root exudates. (A) MRM metabolite detection multi-peak graph in ESI+ mode. (B) MRM metabolite detection multi-peak graph in ESI- mode. The MRM metabolite detection multi-peak diagram in the figure shows the substances that can be detected in the sample, and each mass spectrum peak with different colors represents one metabolite detected. All detected metabolites are displayed in Table S2. (C) Cluster analysis of metabolites from samples of KR1326 and K1076 root exudates. The color indicates the level of accumulation of each metabolite, from low (green) to high (red). The Z-score represents the deviation from the mean by standard deviation units. (D) The classification of identified metabolites. In total, 675 metabolites are divided into 11 categories, different colors represent different categories, the numbers represent the proportion of these metabolites in all metabolites. (E) Principal component analysis (PCA) of metabolites identified from root exudates of KR1326 and K1076. Equal volumes root exudates samples of KR1326 and K1076 were mixed for use as a quality control (Mix).

### 3.3. Identification of Differential Metabolites of Resistant and Susceptible *C. melo* Root Exudates

To reveal the variation in metabolite type and abundance in root exudates of resistant and susceptible *C. melo* cultivars, a qualitative and quantitative analysis and inter-group comparisons of all identified metabolites were carried out. The metabolomics data were analyzed using the OPLS-DA model, and a score map of each group was constructed to further show the differences among the groups (Figure 3A).  $R^2X$ ,  $R^2Y$ , and  $Q^2$  were close to 1, indicating that the model was stable and reliable. To identify differential metabolites, we selected metabolites with an FC  $\geq 2$  (upregulated) or  $\leq 0.5$  (downregulated) with a VIP value  $\geq 1$  from the OPLS-DA model. The statistical analysis identified 213 differential metabolites, including 25 upregulated and 188 downregulated metabolites, in KR1326 compared with K1076 root exudates (Figure 3B). The specific information on differential metabolites is displayed in Figure S4 and Table S3. Furthermore, the number of main metabolite characteristics belonging to each category was analyzed (Figure 3C). There were no upregulated metabolites in the KR1326 root exudates in the categories of lignins and coumarins, organic acids, and terpenoids. In the other metabolite categories, the amount of K1076 metabolites was obviously higher than that of KR1326. In brief, all metabolite categories differentially accumulated in K1076, rather than in KR1326 root exudates.

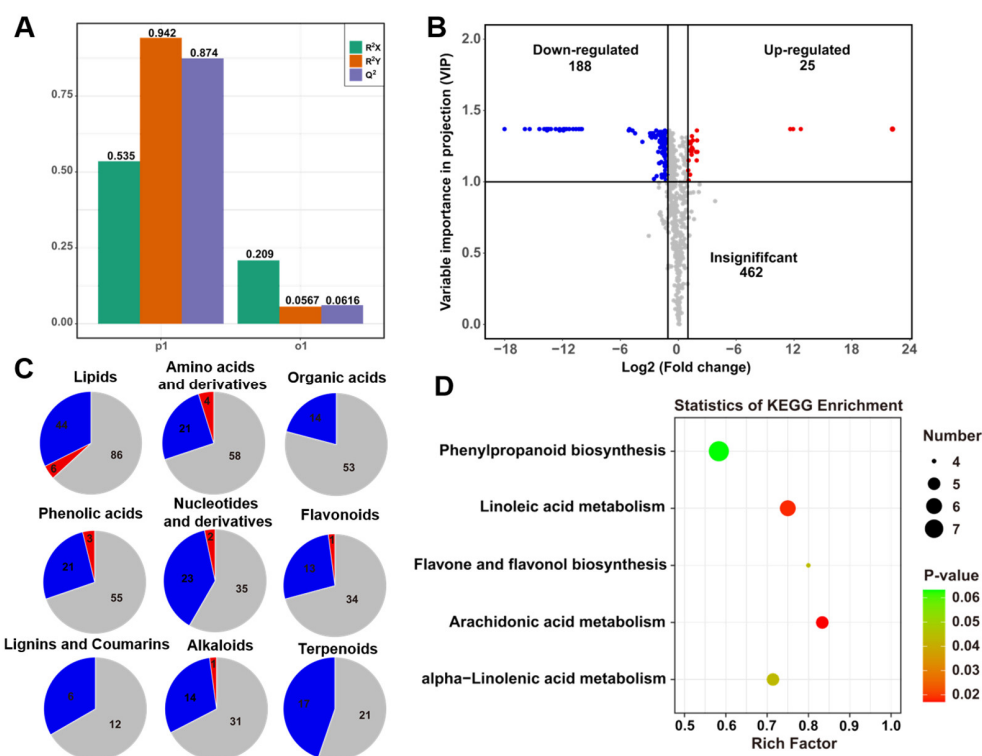


**Figure 3.** Differential metabolites analysis in KR1326 and K1076 root exudates. (A) Score plot of orthogonal partial least squares discriminant analysis (OPLS-DA) model. The model summary diagram shows  $R^2X$ ,  $R^2Y$ , and  $Q^2$  corresponding to the predicted component and orthogonal component in OPLS-DA model. In the abscissa, P1 represents the predicted component, O1 represents the orthogonal component, and the ordinate represents the corresponding  $R^2X$ ,  $R^2Y$ , and  $Q^2$ . (B) Significance analysis of the differential metabolites in the comparison of samples in different cultivars by volcano plot. Differential metabolites were defined as metabolites with Fold change  $\geq 2$  or  $\leq 0.5$  in KR1326 compared to K1076. A threshold of VIP  $\geq 1$  was used to separate differential metabolites from unchanged metabolites. (C) The numbers of up- and down-regulated metabolites in different metabolic categories were shown in pies. Blue region represent down-regulated metabolites; red region represent up-regulated metabolites; grey region represent insignificant metabolites in KR1326 compared with in K1076 root exudates. The number represents the number of corresponding metabolites. (D) KEGG pathways with significant enrichment of differential metabolites.

### 3.4. KEGG Annotation and Enrichment Analysis of Differential Metabolites

According to the KEGG annotation and enrichment results, differential metabolites in KR1326 and K1076 root exudates were enriched in 70 metabolic pathways (Table S4). The KEGG pathways with significant enrichment of differential metabolites are shown in Figure 3D. The differential metabolites were significantly enriched in arachidonic acid metabolism, linoleic acid metabolism, alpha-linolenic acid metabolism, flavone and flavonol biosynthesis, and phenylpropanoid biosynthesis (Figure 3D).

The metabolic pathways of arachidonic acid metabolism, linoleic acid metabolism, and alpha-linolenic acid metabolism were mainly enriched in arachidonic acid, linoleic acid,  $\gamma$ -linolenic acid,  $\alpha$ -linolenic acid, and 17-hydroxylinolenic acid. These were all unsaturated fatty acids, and the relative content of these metabolites in the root exudates of K1076 was higher than that of KR1326 (Figure S3). These metabolites are important energy storage substances in plants, which might be related to physiological differences among resistant and susceptible varieties. The phenylpropanoid biosynthesis pathway enriched 7 metabolites, including p-coumaric acid, p-coumaraldehyde, cinnamic acid, 2-hydroxycinnamic acid, L-phenylalanine, and scopoletin, and their relative contents were higher in root exudates of susceptible *C. melo* cultivar K1076. The flavone and flavonol biosynthesis pathways were enriched with 3-O-methyl quercetin, cosmosiin, vitexin, and isovitexin, which were relatively high in K1076 root exudates.

The metabolic pathways with significant enrichment were found using differential metabolite enrichment analysis, which revealed the potential metabolic pathways of HIFs of *P. aegyptiaca*. These results contributed to finding the HIFs of *P. aegyptiaca* and then applying them to subsequent haustorium induction assays.

### 3.5. Haustorium Induction by Screened Metabolites in Root Exudates

To investigate the role of single metabolites from root exudates in *P. aegyptiaca* haustorium induction and look for HIFs of obligate parasitic plant *P. aegyptiaca*, seven differential metabolites, cytokinins, auxin, ethephon, and DMBQ were selected to test the haustorium induction activity in *P. aegyptiaca*. Root exudates and sterilized water were used as positive and negative controls, respectively. Information on the selected metabolites and commercial compounds is displayed in Table S1.

In this assay, we observed 47.69% haustorium formation using root exudates (the positive control). Predictably, no haustoria were observed in the negative control, and no significant negative effects were observed on the radicle growth of *P. aegyptiaca* under all solvent treatments in the control. The seven selected metabolites, i.e., scopoletin (Scop), quercetin (QC), 4-methoxycinnamic acid (4MCA), cinnamic acid (CA), p-coumaric acid (PA), vanillic acid (VA), and methyl vanillate (MV), showed different haustorium-inducing activities. QC was the most efficient compound, with a maximum activity of 43.33% at  $10^{-3}$  mol/L (Figure S2B), which was not significantly different from the root exudate treatment (Figure 4). DMBQ and Scop treatments also showed relatively high haustorium induction activity, reaching 30% of the haustorium induction rate at the optimal concentration (Figure S2A,M). In addition, 4MCA, VA, and MV induced haustoria at appropriate concentrations (Figure S2C,F,G), while CA and PA were almost inactive in haustorium induction at all concentrations (Figure S2D,E).

To further study the factors affecting the formation of the haustoria, we also studied the effects of various plant hormones on the haustorium formation of *P. aegyptiaca*. Of the cytokinins, i.e., thidiazuron (TDZ), kinetin (KT), N<sup>6</sup>-isopentenyladenosine-D6 (6IP), 6-benzyl aminopurine (6-BA), and zeatin (ZT), 6-BA and ZT showed relatively high activity, with induction activity more than 20% of the optimal concentration (Figure S2H,I). In contrast, the haustorium induction rates of 6IP and KT were almost lower than 12% (Figure S2J,K), and TDZ was almost inactive in haustorium induction at all concentrations (Figure S2L). In addition, the auxin IAA had 40% haustorium induction activity at  $10^{-4}$  mol/L (Figure S2N), which was not significantly different from the root exudate treatment (Figure 4). Exogenous Eth and GA3 treatments showed almost no haustorium induction activity (Figure S2O,P).

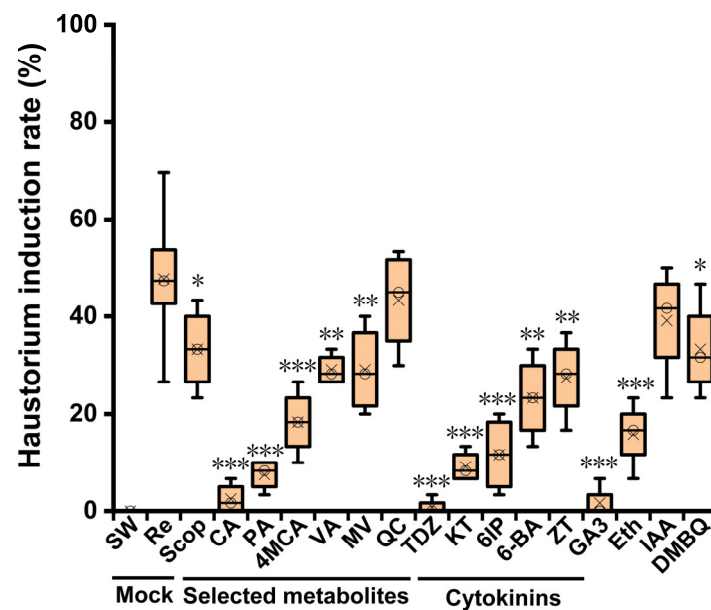


**Figure 4.** The *P. aegyptiaca* haustorium induction rate under each chemical treatment at the optimal concentration. The optimal concentration in each treatment was selected to compare the haustorium induction activity of each screened compound. Germinated *P. aegyptiaca* seeds treated with Scop ( $10^{-6}$  M), CA ( $10^{-5}$  M), PA ( $10^{-6}$  M), 4MCA ( $10^{-5}$  M), VA ( $10^{-4}$  M), MV ( $10^{-4}$  M), QC ( $10^{-3}$  M), TDZ ( $10^{-5}$  M), KT ( $10^{-5}$  M), 6IP ( $10^{-4}$  M), 6-BA ( $10^{-4}$  M), ZT ( $10^{-6}$  M), GA3 ( $10^{-5}$  M), Eth ( $10^{-6}$  M), IAA ( $10^{-4}$  M), and DMBQ ( $10^{-4}$  M) for 7 days, sterilized water and root exudates were used as negative control and positive control, respectively. Each compound is represented by the following abbreviations: SW: sterilized water; Re: root exudates; Scop: scopoletin; CA: cinnamic acid; PCA: p-coumaric acid; 4MCA: 4-methoxycinnamic acid; VA: vanillic acid; MV: methyl vanillate; QC: quercetin; TDZ: thidiazuron; KT: kinetin; 6IP: N6-isopentenyladenosine-D6; 6-BA: 6-Benzyl aminopurine; ZT: zeatin; GA3: gibberellins; ETH: ethephon; IAA: indole-3-acetic acid; DMBQ: 2,6-dimethoxyI-1,4-benzoquinone. Detailed information about the compounds were shown in Table S1. At least three biological replicates per experiment. Asterisks indicate statistically significant differences compared with positive control (Re) using a *t*-test: \*,  $0.01 < p < 0.05$ ; \*\*,  $p < 0.01$ ; \*\*\*,  $p < 0.0001$ . Data represent the mean  $\pm$  SE ( $n > 3$ ).

#### 4. Discussion

*Phelipanche aegyptiaca* is one of the most destructive root parasitic plants of Orobanchaceae, which has significant impacts on crop yields worldwide [27]. However, as an obligate parasite, *P. aegyptiaca* has brought many difficulties to the control work. Effective control methods have become the subject of constant exploration.

Reducing the soil seed bank by inducing suicidal germination of the parasite seeds is an effective method to control the parasite, which has prompted many researchers to study chemicals regulating the germination of parasites. Strigolactones (SLs) are the most potent stimulants and are distributed widely in the plant kingdom [28]. MP3, MP16, and Nijmegen-1, three types of SL analog, the germination induction effect on *Striga hermonthica* is comparable to the standard SL analog GR24, which can be used to improve suicide germination technology [29]. *Brassica napus* exudes only small amounts of SLs, while another active stimulant 2-phenylethyl isothiocyanate (ITC), secreted from root exudates of oilseed rape induced the germination of *P. ramosa* [30]. Besides, the haustorium formation is another key step in the life cycle of parasites after seed germination. It is also significant to study the haustorium formation for understanding the interaction mechanism between the parasite and the host and applying it in the control of the parasite.

At present, research on haustoria mostly focuses on semi-parasitic plants, and the haustorium-inducing factors in holoparasitic plants and the mechanisms of parasitic plants responding to host roots or host root-derived molecules are largely unknown.

*Cucumis melo* is a major host of *P. aegyptiaca*. The resistant cultivar KR1326 and susceptible cultivar K1076 were selected to collect root exudates for seed germination and haustorium induction of *P. aegyptiaca*. Obligate parasite *P. aegyptiaca* can parasitize the whole life cycle of the *C. melo*, including seedling, flowering, and fruiting, and even after the death of the host, *P. aegyptiaca* can still survive for a short time [1]. In contrast, melon at the flowering stage will absorb more nutrients for fruiting, they would grow vigorously and secrete more root exudates. Therefore, *C. melo* at the flowering stage was selected to collect root exudates. In the present study, *C. melo* root exudate extracts stably induced *P. aegyptiaca* seed germination and haustorium formation in vitro (Figure 1), corresponding to previous studies where seeds of parasitic plants from the Orobanchaceae family responded to host root extracts [14,15]. The swelling of the root radicle tip, shorter roots, and outgrowth of epidermal cells were observed in *P. aegyptiaca* after treatment with root exudates or specific chemicals, which were typical haustorium features, which is similar to the description of the characteristics of *Phelipanche* spp. haustoria in previous studies [7,14].

H Haustorium development in Orobanchaceae is not a spontaneous process; it must be stimulated by chemicals secreted by the host roots to initiate the haustorium [1,9]. Almost 50% of *P. aegyptiaca* seeds had induced haustoria after treatment with root exudates, and no haustoria were observed in the control (Figure 4). The results showed that there are special allelochemicals in *C. melo* root exudates that can trigger cell differentiation at the apex of the *P. aegyptiaca* radicle and then form a multicellular early haustorial structure.

To search for allelochemicals related to haustorium induction in root exudates, we compared the induction activity of resistant and susceptible *C. melo* root exudates. Through comparison, we found differences in induction activity between the resistant and susceptible cultivars (Figure 2C,E). Therefore, widely targeted metabolomics based on UPLC MS/MS technology were used to analyze and identify metabolites in root exudates. Notably, 88% of differential metabolites differentially accumulated in K1076 rather than in KR1326 root exudates (Figure 3B), which was closely related to the physiological differences between the two cultivars. The developed size of the root system and plant height of K1076 were significantly higher than KR1326; thus, the K1076 roots secreted more metabolites (Figure S1). The KEGG enrichment analysis confirmed this result, differential metabolites were significantly enriched in arachidonic acid metabolism, linoleic acid metabolism, and alpha-linolenic acid metabolism pathways (Figure 3D); the metabolites in these pathways are mainly important energy storage substances in plants [31], which were all higher in K1076 (Figure S3). In addition, p-coumaric acid, p-coumaraldehyde, p-coumaric alcohol, and cinnamic acid were significantly enriched in the phenylpropanoid biosynthesis pathway. They are all precursors of lignin biosynthesis, and lignin has been reported as an important source of HIFs in semi-parasitic plants [15]. Therefore, we speculated that the phenylpropanoid biosynthesis pathway is closely related to the HIFs of the obligate parasitic plant *P. aegyptiaca*. A previous study indicated that quercetin could inhibit the radicle growth of *P. ramosa* and that 0.05–0.1 mM quercetin and its derivatives had haustorium induction activity [32]. In the present study, 3-O-methyl quercetin was significantly enriched in the flavone and flavonol biosynthesis pathways. Therefore, there are potential HIFs of *P. aegyptiaca* in the flavone and flavonol biosynthesis pathways. These results suggest that these differential metabolites contain HIFs and that different types and contents of HIFs in host exudates result in differences in haustorial induction activity.

Among the different compounds tested in this study, QC and IAA induced haustorium formation with maximum activity similar to *C. melo* root exudate treatment (Figure 4). Quercetin is a flavonoid compound that widely exists in plants, which can adjust polar auxin transport and regulate the activity of various antioxidant enzymes [33]. A recent study showed that quercetin can reduce *P. ramosa* radicle growth and induce haustoria at a concentration range of 0.1–0.05 mM [32]. This is consistent with the results that haustorium formation was observed under QC treatment at  $10^{-3}$ – $10^{-6}$  mol/L in the present study. 3-O-Methylquercetin, a derivative of quercetin, was significantly enriched in K1076 root exudates. This may be associated with its higher haustorium induction rate than with

KR1326. Auxin signaling and transport genes are upregulated in the haustorial tissues of some parasitic plants [34–36]. Exogenous treatment with IAA has been shown to trigger haustorial hair formation in *T. versicolor* [37]. This evidence demonstrates that auxin plays an important role in regulating haustorium development in parasitic plants. Similarly, in the present study, exogenous application of  $10^{-4}$  mol/L IAA treatment displayed relatively high haustorium induction activity, whereas low haustorium induction rates were shown at lower or higher concentrations. A transcriptomic analysis of *P. aegyptiaca* showed that the levels of plant hormone GA3 and ethylene increased after germination stimulation [27]. However, we noticed that the exogenous application of ethylene and GA3 almost did not induce the haustorium formation (Figure S2O,P). This does not mean that GA3 and ethylene do not participate in the regulation of the formation of *P. aegyptiaca*. On the contrary, GA3 and ethylene, and other plant hormones may change endogenously to regulate the growth of *P. aegyptiaca* before parasitism, which is worthy of further study.

Scop and DMBQ also showed relatively high haustorial induction activity. DMBQ, the first HIF identified directly from host root extracts, is a common product of lignin biosynthesis and degradation released by host cells upon host peroxidase activity triggered by hydrogen peroxide production at the tip of *Striga* radicles [9]. At present, it has been widely used in the haustorium induction of semi-parasitic plants. However, the effect of haustoria on obligate parasitic plants has long been uncertain. The results in the present study indicated that *P. aegyptiaca* haustoria can be induced by DMBQ under appropriate conditions, and there is haustorium induction activity at a concentration of  $10^{-4}$ – $10^{-6}$  mol/L (Figure S2M). Other previous studies have confirmed this result. BQ and DMBQ can induce haustorium formation in *Orobancha cumana*, *Orobancha minor*, and *Phelipanche ramosa* [32,38]. Those results demonstrated that DMBQ is also an HIF of obligate-parasitic plants, but the haustorium induction activity is far lower than that of semi-parasitic plants; thus, higher haustorium induction requires further optimization of conditions.

A previous study showed that plant lignin is an important source of HIFs in parasitic plants and that at least one methoxyl group adjacent to the 4-hydroxyl group in phenolics or the 1-oxo group in quinone is an important structural feature of lignin-associated HIFs [15]. PA and CA are important intermediates in lignin biosynthesis, and 4MCA, VA, and MV are their structural analogs [39,40], which are all differential metabolites identified from *C. melo* root exudates and differentially accumulated in K1076 (Table S3). Interestingly, among these metabolites, 4MCA, VA, and MV displayed certain haustorium induction activity, and PA and CA were almost inactive. Compared with material structures, 4MCA, VA, and MV have at least one methoxyl group on the benzene ring, whereas PA and CA do not (Figure 5). These results confirm previous results and suggest that lignin-related compounds are also an important source of HIFs for obligate parasitic plants *P. aegyptiaca*, in which the methoxyl group is an important factor affecting its haustorium induction activity.

In addition, the allelochemicals secreted by the host are necessary for the germination and the formation of the haustorium of parasitic plants. While some hosts with pre-attachment resistance can make themselves “invisible” to parasitic plants by regulating metabolism and changing the type and content of allelochemicals secreted to the outside, or even directly secrete toxic chemicals to inhibit the germination and haustorium formation of parasitic plants, thus avoiding being parasitized [41]. Therefore, studying the metabolic differences between resistant and susceptible hosts is helpful to reveal the mechanism of host resistance and control of parasitic plants.

At present, no haustorium inhibitors were found in this study, while previous studies have shown that exogenous treatment with the auxin activity inhibitor p-chlorophenoxyisobutyric acid (PCIB) or the auxin transport inhibitor 1-N-naphthylphthalamic acid (NPA) dramatically reduces the frequency of infection of *Arabidopsis thaliana* by *P. aegyptiaca* [42]. Tetrafluorobenzoquinone (TFBQ) and Cyclopropyl-p-benzoquinone (CPBQ), the structural analogs of DMBQ, were applied to treat the *Triphysaria versicolor* seeds and reduce the formation of haustorium in the presence of the DMBQ [43]. The results in these studies

indicate that the haustorium inhibitors of the parasitic plant *P. aegyptiaca* may exist, which requires testing more compounds.

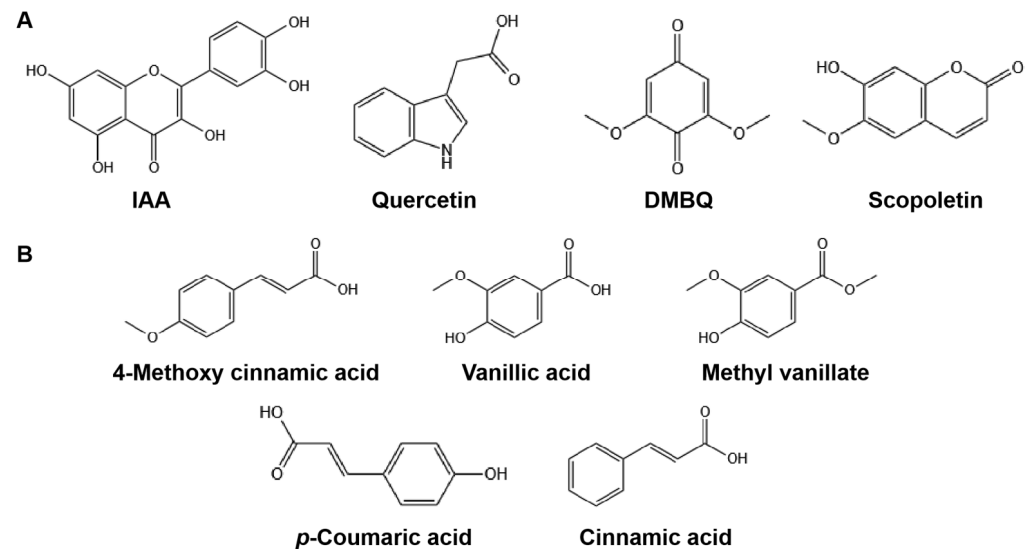


**Figure 5.** Chemical structures of metabolites screened from root exudates of *C. melo* with different haustorium induction activity to *P. aegyptiaca*. **(A)** Metabolites with relatively high haustorium induction activity to *P. aegyptiaca* in this study. **(B)** The presence of a methoxyl group on the benzene ring of 4-methoxy cinnamic acid (4MCA), vanillic acid (VA) and methyl vanillate (MV) shows higher haustorium induction activity than *p*-coumaric acid (PA) and cinnamic acid (CA).

In the present study, quercetin, IAA, and some phenolic acids were screened from the root exudates of *C. melo* and played important roles in inducing haustorium formation in *P. aegyptiaca*. This sheds new light on the mechanism, whereby the host plant first reduces the biosynthesis and secretion of HIFs by applying exogenous inhibitors related to HIFs, and then reduces haustorium formation to avoid the parasitism of *P. aegyptiaca*, which provides effective control methods against parasitic weeds.

**Supplementary Materials:** The following supporting information can be downloaded at: <https://www.mdpi.com/article/10.3390/agronomy13010128/s1>, Figure S1: The differences between susceptible (K1076) and resistant (KR1326) *Cucumis melo* L. cultivars.; Figure S2: Haustorium induction rate under each chemical treatment; Figure S3: Heatmap of differential metabolites in metabolic pathways with significant enrichment; Figure S4: Heatmap of all differential metabolites in resistant and susceptible *C. melo* (KR1326 and K1076) root exudates; Table S1: The information of selected metabolites and compounds used for haustorium induction; Table S2: The information of all identified metabolites; Table S3: Information of the differential metabolites in KR1326 and K1076; Table S4: KEGG classification and enrichment analysis of differential metabolites; Table S5: The composition of Hoagland medium for hydroponic culture.

**Author Contributions:** P.B., S.Z. and X.Z. designed the research. P.B., C.S. and X.C. performed the experiments. P.B., C.S. and Z.Y. performed the data analysis and interpretation. P.B., S.Z. and X.Z. wrote the manuscript. All authors have read and agreed to the published version of the manuscript.

**Funding:** This work was supported by National Natural Science Foundation of China [grant numbers 32160649, 31460467]; XPCC fund [grant numbers 2018CB022].

**Data Availability Statement:** Not applicable.

**Acknowledgments:** We are grateful to Xinli Ma for providing seeds of melon cultivars, including the KR1326 and K1076.

**Conflicts of Interest:** The authors declare no conflict of interest.

## References

1. Joel, D.M. *Parasitic Orobanchaceae: Parasitic Mechanisms and Control Strategies*; Springer: Berlin/Heidelberg, Germany, 2013; pp. 313–344. [[CrossRef](#)]
2. Chris, P. Parasitic weeds: A world challenge. *Weed Sci.* **2012**, *60*, 269–276. [[CrossRef](#)]
3. Parker, C. Observations on the current status of *Orobanche* and *Striga* problems worldwide. *Pest Manag. Sci.* **2009**, *65*, 453–459. [[CrossRef](#)]
4. Yao, Z.Q.; Cao, X.L.; Fu, C.; Zhao, S.F. Review of the distribution and management technology of various *Orobanche* L. species in Xinjiang, China. *J. Biosaf.* **2017**, *26*, 23–29.
5. Zhang, X.K.; Yao, Z.Q.; Zhao, S.F.; Ding, L.L.; Du, J. Distribution, harmfulness and its assessment of *Orobanche aegyptiaca* in Xinjiang province. *Phytosanitary* **2012**, *26*, 31–33.
6. Delavault, P. Knowing the parasite: Biology and genetics of *Orobanche*. *Helia* **2015**, *38*, 15–29. [[CrossRef](#)]
7. Yoshida, S.; Cui, S.; Ichihashi, Y.; Shirasu, K. The haustorium, a specialized invasive organ in parasitic plants. *Annu. Rev. Plant Biol.* **2016**, *67*, 643–667. [[CrossRef](#)] [[PubMed](#)]
8. FernándezAparicio, M.; Delavault, P.; Timko, M.P. Management of infection by parasitic weeds: A review. *Plants* **2020**, *9*, 1184. [[CrossRef](#)]
9. Delavault, P.; Montiel, G.; Brun, G.; Pouvreau, J.B.; Thoiron, S.; Simier, P. Communication between host plants and parasitic plants. *Acad. Press* **2017**, *82*, 55–82. [[CrossRef](#)]
10. Aly, R. Trafficking of molecules between parasitic plants and their hosts. *Weed Res.* **2013**, *53*, 231–241. [[CrossRef](#)]
11. Aly, R.; Hamamouch, N.; Abu-Nassar, J.; Wolf, S.; Joel, D.M.; Eizenberg, H.; Kaisler, E.; Cramer, C.; Gal-On, A.; Westwood, J.H. Movement of protein and macromolecules between host plants and the parasitic weed *Phelipanche aegyptiaca* Pers. *Plant Cell Rep.* **2011**, *30*, 2233–2241. [[CrossRef](#)]
12. Clarke, C.R.; Park, S.Y.; Tuosto, R.; Jia, X.Y.; Yoder, A.; Mullekom, J.V.; Westwood, J. Multiple immunity-related genes control susceptibility of *Arabidopsis thaliana* to the parasitic weed *Phelipanche aegyptiaca*. *PeerJ* **2020**, *8*, e9268. [[CrossRef](#)]
13. Goyet, V.; Wada, S.; Cui, S.; Wakatake, T.; Shirasu, K.; Montiel, G.; Simier, P.; Yoshida, S. Haustorium inducing factors for parasitic Orobanchaceae. *Front. Plant Sci.* **2019**, *10*, 1056. [[CrossRef](#)] [[PubMed](#)]
14. Goyet, V.; Billard, E.; Pouvreau, J.; Lechat, M.; Pelletier, S.; Bahut, M.; Monteau, F.; Spíchal, L.; Delavault, P.; Montiel, G.; et al. Haustorium initiation in the obligate parasitic plant *Phelipanche ramosa* involves a host-exudated cytokinin signal. *J. Exp. Bot.* **2017**, *68*, 5539–5552. [[CrossRef](#)]
15. Cui, S.; Wada, S.; Tobimatsu, Y.; Takeda, Y.; Saucet, S.B.; Takano, T.; Umezawa, T.; Shirasu, K.; Yoshida, S. Host lignin composition affects haustorium induction in the parasitic plants *Phtheirospermum japonicum* and *Striga hermonthica*. *New Phytol.* **2018**, *218*, 710–723. [[CrossRef](#)]
16. Aoki, N.; Cui, S.; Yoshida, S. Cytokinins induce prehaustoria coordinately with quinone signals in the parasitic plant *Striga hermonthica*. *Plant Cell Physiol.* **2022**, *63*, 1446–1456. [[CrossRef](#)] [[PubMed](#)]
17. Wang, Y.; Murdock, M.; Lai, S.; Steele, D.B.; Yoder, J. Kin recognition in the parasitic plant *Triphysaria versicolor* is mediated through root exudates. *Front. Plant Sci.* **2020**, *11*, 560682. [[CrossRef](#)]
18. Fernández-Aparicio, M.; Reboud, X.; Gibot-Leclerc, S. Broomrape weeds. Underground mechanisms of parasitism and associated strategies for their control: A review. *Front. Plant Sci.* **2016**, *7*, 135. [[CrossRef](#)] [[PubMed](#)]
19. Fernández-Aparicio, M.; Masi, M.; Maddau, L.; Cimmino, A.; Evidente, M.; Rubiales, D.; Evidente, A. Induction of haustorium development by sphaeropsidones in radicles of the parasitic weeds *Striga* and *Orobanche*. A structure-activity relationship study. *J. Agric. Food Chem.* **2016**, *64*, 5188–5196. [[CrossRef](#)] [[PubMed](#)]
20. Wakatake, T.; Ogawa, S.; Yoshida, S.; Shirasu, K. An auxin transport network underlies xylem bridge formation between the hemi-parasitic plant *Phtheirospermum japonicum* and host *Arabidopsis*. *Development* **2020**, *147*, dev.187781. [[CrossRef](#)]
21. Cui, S.; Kubota, T.; Nishiyama, T.; Ishida, J.; Shigenobu, S.; Shibata, T.; Toyoda, A.; Hasebe, M.; Shirasu, K.; Yoshida, S. Ethylene signaling mediates host invasion by parasitic plants. *Sci. Adv.* **2020**, *6*, eabc2385. [[CrossRef](#)]
22. Kokla, A.; Leso, M.; Zhang, X.; Simura, J.; Serivichyaswat, P.; Cui, S.; Ljung, K.; Yoshida, S.; Melnyk, C. Nitrogen represses haustoria formation through abscisic acid in the parasitic plant *Phtheirospermum japonicum*. *Nat. Commun.* **2022**, *13*, 2976. [[CrossRef](#)] [[PubMed](#)]
23. Wada, S.; Cui, S.; Yoshida, S. Reactive oxygen species (ROS) generation is indispensable for haustorium formation of the root parasitic plant *Striga hermonthica*. *Front. Plant Sci.* **2019**, *10*, 328. [[CrossRef](#)] [[PubMed](#)]
24. Laohavisit, A.; Wakatake, T.; Ishihama, N.; Mulvey, H.; Takizawa, K.; Suzuki, T.; Shirasu, K. Quinone perception in plants via leucine-rich-repeat receptor-like kinases. *Nature* **2020**, *7832*, 92–97. [[CrossRef](#)] [[PubMed](#)]
25. Chen, Y.; Kuang, Y.; Shi, L.; Wang, X.; Fu, H.; Yang, S.; Sampietro, D.A.; Huang, L.; Yuan, Y. Synthesis and evaluation of new halogenated GR24 analogs as germination promoters for *Orobanche cumana*. *Front. Plant Sci.* **2021**, *12*, 725949. [[CrossRef](#)]
26. Nelson, D.C. The mechanism of host-induced germination in root parasitic plants. *Plant Physiol.* **2021**, *185*, 1353–1373. [[CrossRef](#)]
27. Yao, Z.; Tian, F.; Cao, X.; Xu, Y.; Chen, M.X.; Xiang, B.C.; Zhao, S.F. Global transcriptomic analysis reveals the mechanism of *Phelipanche aegyptiaca* seed germination. *Int. J. Mol. Sci.* **2016**, *17*, 1139. [[CrossRef](#)]
28. Xie, X.; Yoneyama, K.; Yoneyama, K. The strigolactone story. *Annu. Rev. Phytopathol.* **2010**, *48*, 93–117. [[CrossRef](#)]

29. Jamil, M.; Wang, J.Y.; Yonli, D.; Ota, T.; Berqdar, L.; Traore, H.; Margueritte, O.; Zwanenburg, B.; Asami, T.; Al-Babili, S. *Striga hermonthica* suicidal germination activity of potent strigolactone analogs: Evaluation from laboratory bioassays to field trials. *Plants* **2022**, *11*, 1045. [[CrossRef](#)]
30. Miura, H.; Ochi, R.; Nishiwaki, H.; Yamauchi, S.; Xie, X.N.; Nakamura, H.; Yoneyama, K.; Yoneyama, K. Germination stimulant activity of isothiocyanates on *Phelipanche* spp. *Plants* **2022**, *11*, 606. [[CrossRef](#)]
31. Gah-Hyun, L.; Richa, S.; Aardra, K.; Pradeep, K. Fatty acid- and lipid- mediated signaling in plant defense. *Annu. Rev. Phytopathol.* **2017**, *55*, 505–536. [[CrossRef](#)]
32. FernándezAparicio, M.; Masi, M.; Cimmino, A.; Vilariño, S.; Evidente, A. Allelopathic effect of quercetin, a flavonoid from *Fagopyrum esculentum* Roots in the Radicle Growth of *Phelipanche ramosa*: Quercetin natural and semisynthetic analogues were used for a structure-activity relationship investigation. *Plants* **2021**, *10*, 543. [[CrossRef](#)]
33. Singh, P.; Arif, Y.; Bajguz, A.; Hayat, S. The role of quercetin in plants. *Plant Physiol. Biochem.* **2021**, *166*, 10–19. [[CrossRef](#)] [[PubMed](#)]
34. Zhang, X.; Berkowitz, O.; Teixeira, D.S.J.A.; Zhang, M.H.; Ma, G.H.; Whelan, J.; Duan, J. RNA-Seq analysis identifies key genes associated with haustorial development in the root hemiparasite *Santalum album*. *Front. Plant Sci.* **2015**, *6*, 661. [[CrossRef](#)] [[PubMed](#)]
35. Ranjan, A.; Ichihashi, Y.; Farhi, M.; Zumstein, K.; Townsley, B.; David-Schwartz, R.; Sinha, N.R. De novo assembly and characterization of the transcriptome of the parasitic weed dodder identifies genes associated with plant parasitism. *Plant Physiol.* **2014**, *166*, 1186–1199. [[CrossRef](#)]
36. Chen, L.L.; Guo, Q.S.; Zhu, Z.B.; Wan, H.F.; Zhang, H. Integrated analyses of the transcriptome and small RNA of the hemiparasitic plant *Monochasma savatieri* before and after establishment of parasite-host association. *BMC Plant Biol.* **2021**, *21*, 90. [[CrossRef](#)] [[PubMed](#)]
37. Tomilov, A.A.; Tomilova, N.B.; Abdallah, I.; Yoder, J. Localized hormone fluxes and early haustorium development in the hemiparasitic plant *Triphysaria versicolor*. *Plant Physiol.* **2005**, *138*, 1469–1480. [[CrossRef](#)] [[PubMed](#)]
38. Bar-Nun, N.; Sachs, T.; Mayer, A.M. A role for IAA in the infection of *Arabidopsis thaliana* by *Orobanche aegyptiaca*. *Ann. Bot.* **2008**, *101*, 261–265. [[CrossRef](#)] [[PubMed](#)]
39. Fernández-Aparicio, M.; Masi, M.; Cimmino, A.; Evidente, A. Effects of benzoquinones on radicles of *Orobanche* and *Phelipanche* species. *Plants* **2021**, *10*, 746. [[CrossRef](#)] [[PubMed](#)]
40. Dong, N.; Lin, H. Contribution of phenylpropanoid metabolism to plant development and plant-environment interactions. *J. Integr. Plant Biol.* **2020**, *63*, 180–209. [[CrossRef](#)]
41. Jhu, M.; Sinha, N.R. Parasitic plants: An overview of mechanisms by which plants perceive and respond to parasites. *Annu. Rev. Plant Biol.* **2022**, *73*, 433–455. [[CrossRef](#)]
42. Marchiosi, R.; Dos Santos, W.D.; De Lima, R.B.; Soares, A.R.; Finger-Teixeira, A.; Mota, T.R.; De Oliveira, D.M.; Foletto-Felipe, M.D.; Abrahao, J.; Ferrarese, O. Biosynthesis and metabolic actions of simple phenolic acids in plants. *Phytochem. Rev.* **2020**, *19*, 865–906. [[CrossRef](#)]
43. Wang, Y.; Steele, D.; Murdock, M.; Lai, S.; Yoder, J. Small-molecule screens reveal novel haustorium inhibitors in the root parasitic plant *Triphysaria versicolor*. *Phytopathology* **2019**, *109*, 1878–1887. [[CrossRef](#)] [[PubMed](#)]

**Disclaimer/Publisher’s Note:** The statements, opinions and data contained in all publications are solely those of the individual author(s) and contributor(s) and not of MDPI and/or the editor(s). MDPI and/or the editor(s) disclaim responsibility for any injury to people or property resulting from any ideas, methods, instructions or products referred to in the content.